Utah State University

January 1, 2012

The Density Factor in the Synthesis of Carbon Nanotube Forest by Injection Chemical Vapor Deposition

R. W. Call
C. G. Read
C. Mart
T. -C. Shen, *Utah State University*

The density factor in the synthesis of carbon nanotube forest by injection chemical vapor deposition

R. W. Call, C. G. Read, C. Mart, and T.-C. Shen

Articles you may be interested in

Diameter and wall number control of carbon nanotubes by chemical vapor deposition
J. Appl. Phys. **114**, 244302 (2013); 10.1063/1.4851656

Multiwalled Carbon Nanotube Forest Grown via Chemical Vapor Deposition from Iron Catalyst Nanoparticles, by XPS
Surf. Sci. Spectra **20**, 62 (2013); 10.1116/11.20121103

Effect of parameters on carbon nanotubes grown by floating catalyst chemical vapor deposition
AIP Conf. Proc. **1502**, 242 (2012); 10.1063/1.4769148

Nucleation and growth of carbon nanotubes in catalytic chemical vapor deposition
J. Appl. Phys. **102**, 044303 (2007); 10.1063/1.2769354

Carbon nanotubes synthesized by Ni-assisted atmospheric pressure thermal chemical vapor deposition
J. Appl. Phys. **91**, 3847 (2002); 10.1063/1.1448877

The density factor in the synthesis of carbon nanotube forest by injection chemical vapor deposition

R. W. Call, C. G. Read, C. Mart, and T.-C. Shen
Department of Physics, Utah State University, Logan, Utah 84322, USA

Beneath the seeming straight-forwardness of growing carbon nanotube (CNT) forests by the injection chemical vapor deposition (CVD) method, control of the forest morphology on various substrates is yet to be achieved. Using ferrocene dissolved in xylene as the precursor, we demonstrate that the concentration of ferrocene and the injection rate of the precursor dictate the CNT density of these forests. However, CNT density will also be affected by the substrates and the growth temperature which determine the diffusion of the catalyst adatoms. The CNT growth rate is controlled by the temperature and chemical composition of the gases in the CVD reactor. We show that the final height of the forest is diffusion limited, at least in the conditions of our experiments. Because of the proximity and entanglement of the CNTs in a forest, the growing CNTs can lift-up the inactive CNTs resulting in reduced density toward the base of the forest unless the nucleation rate of the new catalyst particles is sufficiently high to replenish the inactive catalyst particles. Significant loss of CNT attachment by the lift-up effect reduces the adhesion of the forest to the substrate. Optimizing the ferrocene concentration in the precursor, precursor injection rate, gas mixture, substrate, and temperature is necessary to achieve desired forest morphology for specific applications. © *2012 American Institute of Physics*. [http://dx.doi.org/10.1063/1.4768928]

I. INTRODUCTION

The synthesis of a layer of either single-walled or multi-walled carbon nanotube (CNT) forests with more than mm-height has been intensively studied and achieved by many groups in the past decade.[1,2] Thermal chemical vapor deposition (CVD) has proved to be the most efficient method to produce large scale, substrate-bonded CNT forests with high carbon purity, alignment, surface area, and growth rate. Within the CVD approach, a layer of catalyst particles (usually from transition metals) can be deposited on a substrate before the introduction of carbon source gases, known as the catalyst pre-deposition method,[3] or the catalyst precursor can be injected into the reactor at the same time with carbon source gases, known as the injection CVD,[4] floating catalyst,[5] spray pyrolysis,[6] aerosol-assisted catalytic CVD,[7] or continuous-feed CVD.[8] The advantage of the catalyst pre-deposition method is that it allows control of the catalyst particle density and size distribution which are highly dynamical throughout the CVD process and are critical to the CNT forest morphology. The common way to deposit a layer of catalyst particle on the substrate is by evaporating or sputtering a pure metal source, but it is also possible to spin-coat iron compounds[9,10] or deposit colloidal iron oxide and aluminum ferrite nanocrystal solutions[11] on the substrate. It was found early on that the catalyst particle sizes can be controlled by the metal film thickness.[12–14] Later works clearly revealed that morphology of the catalyst particles continues to evolve in elevated temperatures either in pre-synthesis annealing[15] and/or during synthesis.[16] From transmission electron microscopy[17,18] and the correlation between the densities of single-walled CNTs and catalyst particles,[19] it can be established that in CVD each CNT originates from a single catalyst particle, if the particle is sufficiently small.

With appropriate choices of catalyst, underlayer, gas mixture, and a small amount of water, a "super growth" rate of 250 μm/min for single-walled CNT forests has been demonstrated.[20] The intricate physics and chemistry involved in the catalyst particles evolution in the CVD process has since been extensively investigated.[21–25] Control of catalyst pre-deposition CVD as demonstrated by the synthesis of A4-sized single-walled CNT forests[2] and the continuous production of multi-walled CNT forests[26] presents potential technologies toward industrial-scale productions.

Control of injection CVD, however, has not been as developed as its catalyst pre-deposition counterpart. The main challenge is again in the control of the catalyst particle size and density. The common catalyst precursors in injection CVD are based on a metallocene dissolved in a hydrocarbon solvent.[27–29] Since the pyrolysis of the precursor in the CVD reactor provides both the catalyst and carbon source, the catalyst particles are continuously nucleated and resupplied as CNTs are synthesized. Depending on the temperature the pyrolysis of the metallocene and the hydrocarbon solvent can generate toluene and benzene,[30,31] which further complicates the pyrolysis of simple hydrocarbons such as methane[32] used in catalyst pre-deposition CVD. Additionally, the nucleation of catalyst particles simultaneously with carbon diffusion and precipitation affects nanoparticle dynamics including particle agglomeration, adatoms subsurface diffusion, and the competition between the growth of graphitic carbon and amorphous carbon on catalyst surfaces. Although an average growth rate of 50 μm/min has been reported,[33] the more common growth rate by injection CVD is much less than that and no synthesis of single-walled CNT forest has been reported. However, for applications, such as superhydrophobic surfaces,[34] thermal interface materials,[35] ultra-black surfaces,[36] dry adhesives,[37]

112, 124303-1

composites,[38] or fuel cells,[39] where the superiority of a particular type of CNT has not been observed, the one-step synthesis of multi-walled CNT forests by injection CVD is still appealing. Since there is a continuous feed of the catalyst during injection CVD, it is conceivable that the metallocene concentration in the precursor, the injection rate of the precursor, and the temperature can control the nanoparticle size and density. Indeed, several studies have reported tube diameters, forest height, and mass densities in terms of these growth parameters.[4,41–43] However, because of the multidimensional parameter space and different experimental setups, these results are not all consistent. In particular most of the studies use forest height as the figure of merit to evaluate their growth conditions. Nanotube density in a forest is much harder to measure because of the three-dimensional entangled nature of the forest. Even removing the forest physically or chemically to count the catalyst particles cannot reveal the true CNT density because only a fraction of the catalyst particles actually grow CNTs.[19] Recently, using spatially resolved x-ray scattering to measure CNT density prepared by catalyst pre-deposition method shows that the nanotube density is closely related to the forest growth and termination mechanism.[44]

In this paper, we report the effect of CNT density on forest morphologies and the density correlation with ferrocene concentration in the precursor, the precursor injection rate, hydrogen concentration, growth temperature, and substrates. Because trace amount of gas impurities can lead to significant morphology variations,[45] it is unlikely to have a universal recipe to achieve certain desired density and height of multi-walled CNT forests by injection CVD method. However, we hope that our analyses contribute to the physical understanding of the CNT forest morphology and help generate setup-dependent recipes to customize morphologies for applications.

II. EXPERIMENTAL

All experiments were conducted in a 1 in. OD quartz reactor in a 36 in. long single-zone atmospheric pressure tube furnace. The total flow rate of the carrier gas was maintained at 100 sccm (cubic centimeters per minute at standard temperature and pressure). The substrates are laid horizontally, parallel to the direction of gas flow, on a 1/8 in. thick quartz plate near the center of the reactor. The reactor was first pumped down to 3×10^{-2} Torr at room temperature before flowing in ultrapure Ar gas at 10 psi above the ambient. The reactor maintains a positive pressure by flowing in Ar and other gas mixtures during temperature ramping-up and cooling-down phase and CNT synthesis. The precursor is ferrocene dissolved in xylene at concentrations of 1.5, 3.0, 6.0, and 7.2 mol. %. The carrier gas is Ar mixed with various fractions of ultrapure H_2 at a total flow rate of 100 sccm. The precursor was fed into a stainless steel injector by a syringe pump at a flow rate of either 2 ml/h or 4 ml/h. The injector was on a mobile stage to maintain its temperature at ∼175 °C near the front part of the quartz reactor. The precursor vapor and the carrier gas were mixed in the injector before being blown into the reactor. In this report, we will compare CNT

forest growth from three kinds of substrate: fused quartz, silicon with thermal oxide up to 470 nm, and sapphire with polished but random oriented surfaces. The quartz and silicon samples are rectangular about 1 cm on the side. The sapphire samples are 0.5 mm thick disks with 6 mm diameter. In this report, we only analyze CNT growth at 700 °C and 760 °C to delineate temperature effects. To study substrate effects, different substrates were placed side by side on the quartz plate at the same distance from the injector to reduce any precursor depletion along the flow.

The morphologies of the CNT forests were characterized by scanning electron microscopy (SEM). The height of the forest was determined from the side-view images of many notches cut with a razor blade along the edges of the forests. However, the cleaved edges of quartz and silicon and polished edges of sapphire often lead to different growth morphologies; cutting notches often smears the forests at the top and the torn sections often result in greater heights than the original forest. Therefore, ranges of height instead of mean values are presented in this paper. Nevertheless, we find that a clear trend of heights corresponding to various experimental conditions can be observed.

Because the CNT forest density is relatively uniform across the substrate based on the top view SEM images, the CNT density can be inferred by quantifying the CNT coverage from a series of side-view SEM images from tip to base of each forest. Assuming that the focal depth of SEM is constant at a fixed acceleration voltage and magnification, we use image processing software to create line profiles and a brightness histogram from thin slices of the SEM images perpendicular to the forest growth direction. We then use zoomed-in images to determine the brightness threshold of the CNT "covered" region in that slice. The threshold is applied to the histogram to determine the percentage coverage. This process is repeated for many slices in the same area. By using many small slices instead of one large slice we avoid counting individual CNT multiple times and correct for any average brightness gradient across the image. The results from the slices produce a range that represents the CNT percentage coverage of the forest at a particular distance from the substrate. Clearly, the percentage coverage is not as quantitative as those densities derived from x-ray[44] or z-contrast transmission electron microscopy,[46] but we believe that it is proportional to local CNT density and provides an additional quantitative characterization of the forest morphology other than the height. In fact, because we have chosen our slices very thin to avoid "multiple counting" of the misaligned CNTs near the base, our percentage coverage is closer to the "number density" than "mass density" of the forest. With this understanding, we will use "density" in place of percentage coverage hereafter.

III. RESULTS AND DISCUSSION

A. Substrate effect on CNT forest density

Figure 1 illustrates that the CNT forests grown on a sapphire substrate are visibly denser and hence more aligned than those grown on a quartz substrate under identical growth conditions. When annealing 10-nm Fe films on either Al_2O_3 or SiO_2 substrates at 750 °C in an Ar/H_2 ambient,
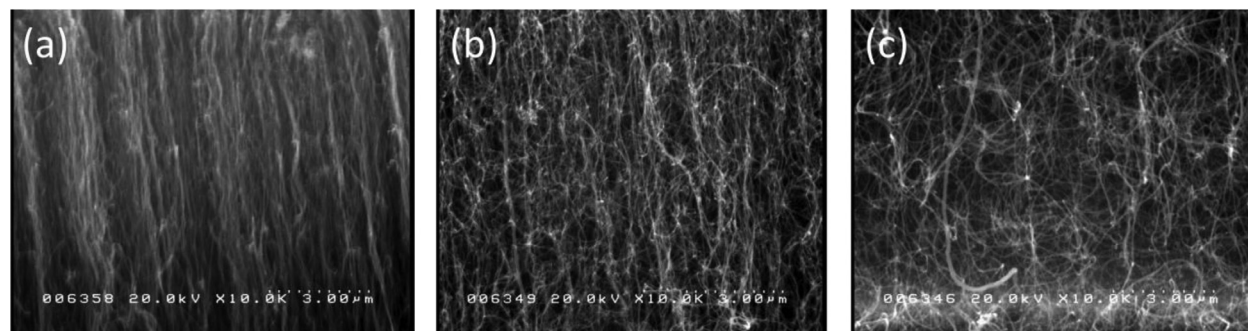
FIG. 1. CNT forest grown at 760 °C by 1.5 mol. % ferrocene/xylene injected at 4 ml/h for a total of 0.5 ml. The carrier gas mixture was H_2:Ar = 50:50 sccm. (a) Tip region of the forest on sapphire. (b) Tip and (c) base region of the forest on quartz.

Mattevi *et al.* reported that Fe particles on SiO_2 are much larger and sparse while those on Al_2O_3 are smaller and denser.[21] Sapphire is a single crystal alumina. Ohno *et al.* showed that Co nanoparticles evolve similarly on SiO_2 and sapphire substrates.[47] These observations suggest that the interaction between Fe and Al_2O_3 is much stronger than Fe and SiO_2. Consequently, Fe atoms can diffuse much faster on and into the SiO_2 substrate resulting in loss or agglomeration of the catalyst particles and thus, less dense CNTs. Our results indicate that this scenario is applicable also to injection CVD where nanoparticles are continuously forming and evolving.

However, we also observed that the heights of CNT forests on sapphire are more than a factor of 2 lower than those grown on quartz under the same conditions as shown in Fig. 2. This is in contradiction to a recent report by Di *et al.* who found that using similar growth condition as Mattevi *et al.* the CNT forests grown on Al_2O_3 have a higher growth rate than on SiO_2.[48] The discrepancy presents an interesting difference between the CNT growth by injection CVD and by catalyst pre-deposition CVD. Because of the continuous injection of ferrocene during CNT synthesis, the loss of Fe

FIG. 2. CNT forests grown at 700 °C on quartz (open), and sapphire (filled) for different H_2:Ar ratios in the carrier gas. The total flow rate was kept at 100 sccm. The precursor was 1.5 mol. % ferrocene/xylene injected at 2 ml/h for a total of 0.5 ml.

adatoms through subsurface diffusion, encapsulation into the cavity of the CNT,[18,49] and Ostwald ripening[16] can be counteracted by the newly arrived Fe adatoms. Therefore, the factors suppressing the CNT growth on SiO_2 are not as limiting as in the pre-deposited catalyst method. In fact, if not properly adjusted, the density of the catalyst particles can be sufficiently high to incur a diffusion limit which leads to lower forest heights on sapphire, because the CNTs in our system grow from the base. The base growth mode was determined from sequential growth experiments and is consistent with many earlier reports using ferrocene solutions.[7,50] The diffusion limit will be discussed more in Sec. III C.

The notion of CNT forest density depending on substrate is further supported by a series of forest growths on Si substrates with different oxide thickness. It has been reported that the height of CNT forests depends on the oxide thickness up to 50 nm.[51] The low growth is not because of any reduction of the reaction rates in CNT growth at catalyst particle surfaces but because of the loss of catalyst particles due to the diffusion of Fe through the silicon oxide.[52] This scenario is confirmed by measuring the density of the CNT forests at both the tip and the base region of different oxide surfaces as shown in Fig. 3. Lower oxide thickness leads to more diffusion loss of the catalyst and thus, less CNT density. Figure 3 also indicates that the density at the base is consistently less than the density at the tip. This phenomenon can be explained by the following scenario. Once the nanoparticle is consumed by diffusing into the substrate or being encapsulated in the CNT cavity,[50] the CNT ceases to grow from the base. If through entanglement the growing CNTs create sufficient force to lift-up those terminated CNTs, the density near the base will be reduced. Note, however, that in this case lower density does not lead to higher height. The precursor diffusion through the existing forest is not the rate limiting step in these experiments, because ferrocene concentration in these experiments was low and the forests were not very tall. Instead, the height of a forest is dictated by the rate of new catalyst particle nucleation to grow new CNTs to lift up the CNTs from inactive catalyst particles.[7,18]
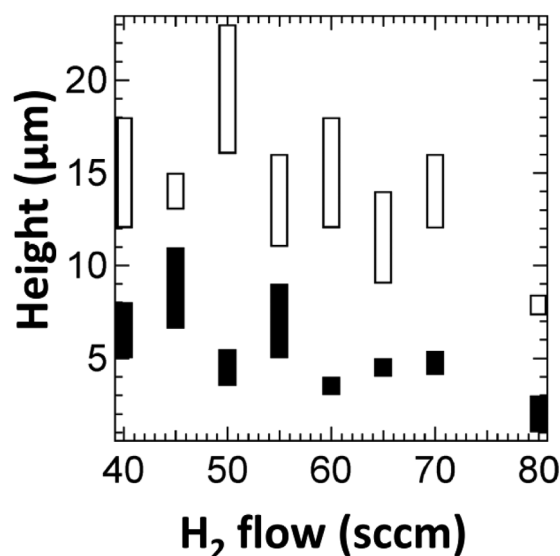
B. CNT density varies along the forest growth direction

Because catalyst particles nucleate continuously on the substrate from the supply of ferrocene, the density of CNT
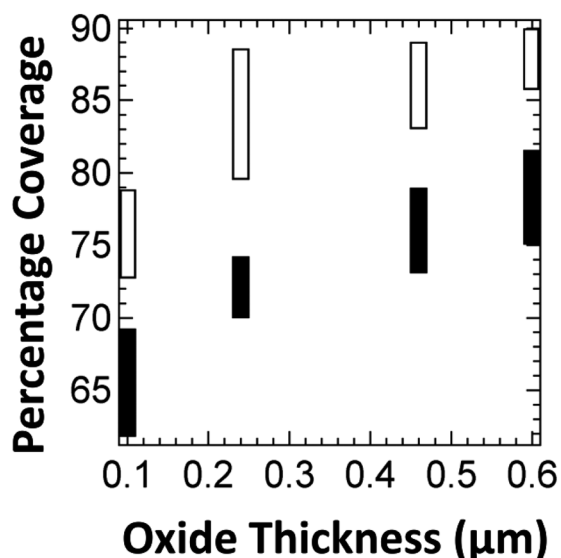
FIG. 3. Percentage coverage of the tip (open) and base (filled) of CNT forests grown at 700 °C on Si with different SiO$_2$ thickness. The forest height from the thinnest to thickest oxide is 75–100 μm, 30–40 μm, 63–70 μm, and 60–70 μm, respectively. The carrier gas was H$_2$:Ar = 50:50 sccm. The precursor was 1.5 mol. % ferrocene/xylene injected at 2 ml/h for a total of 2.4 ml.

FIG. 5. Percentage coverage of CNT from the substrate in forests grown at 700 °C with a carrier gas of H$_2$:Ar = 50:50 sccm by a precursor of 3 mol. % ferrocene/xylene (open) injected at 2 ml/h for a total of 3.4 ml and a precursor of 1.5 mol. % ferrocene/xylene (filled) injected at 2 ml/h for a total of 2.4 ml.

could increase with time and the density at the base could be higher than that at the tip as opposed to the observed density decay toward the base in the catalyst pre-deposition cases.[44] However, comparing Figs. 1(b) with 1(c) clearly reveals the opposite. In fact, the base density is further reduced if we switch the carbon feedstock from ferrocene to ethylene without interruption during synthesis as depicted in Fig. 4. Clearly, the continuous injection of Fe can influence the CNT density. Figure 5 shows the density variation from the base to the tip of CNT forests grown by 1.5 mol. % and 3 mol. % ferrocene precursor, respectively. The density from the 3% ferrocene concentration is higher but not by a factor of 2 than those from 1.5% by our counting algorithm. Even using a ferrocene concentration of 6% and 7.2% (saturation), we did not observe any sign of increasing CNT density from tip to base. Furthermore, these high concentration precursors lead to very short and defective CNT forests which will be discussed in Sec. III C.

Van der Waals forces due to proximity and interlocking through entanglement among adjacent CNTs are the main
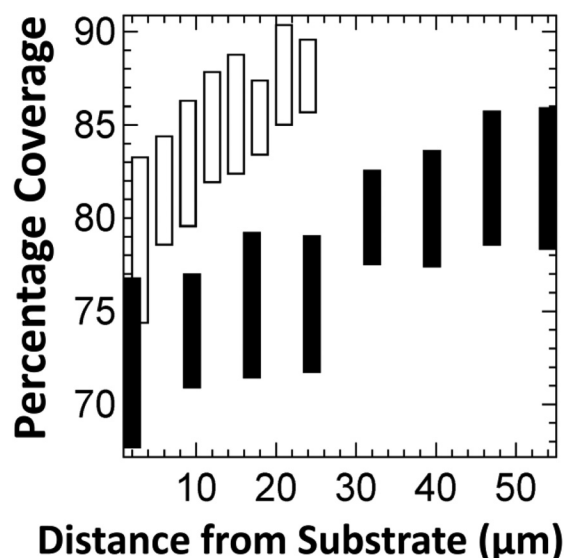
reasons that CNT growth can be vertically "aligned," appear to have the same height in a forest,[53] be terminated abruptly (in some case),[54] and lose alignment near the base.[16,55] In the case of pre-deposited catalyst, the number of nanoparticles can only decrease due to catalyst adatoms diffusion and being encapsulated into the CNT cavity. When a nanoparticle can no longer decompose hydrocarbon molecules to sustain the CNT growth, the adjacent active CNTs can lift up the terminated CNT thus reducing the CNT density toward the base. It is conceivable that with a proper catalyst supply rate, which is related to the catalyst lifetime, the newly nucleated nanoparticles and their CNTs can continue the forest growth forever. Indeed, while we find that higher ferrocene concentration leads to a higher density gradient toward the base and earlier termination of the forest growth, Li *et al.* achieve 1.5-cm high CNT forest with a ferrocene concentration of merely ~0.65 mol. % to ensure a sufficient supply of carbon and Fe feedstock. Additionally, a small amount of air helped lengthen the catalyst lifetime and enhance the growth rate to 10 μm/min. Of course, low ferrocene concentration in

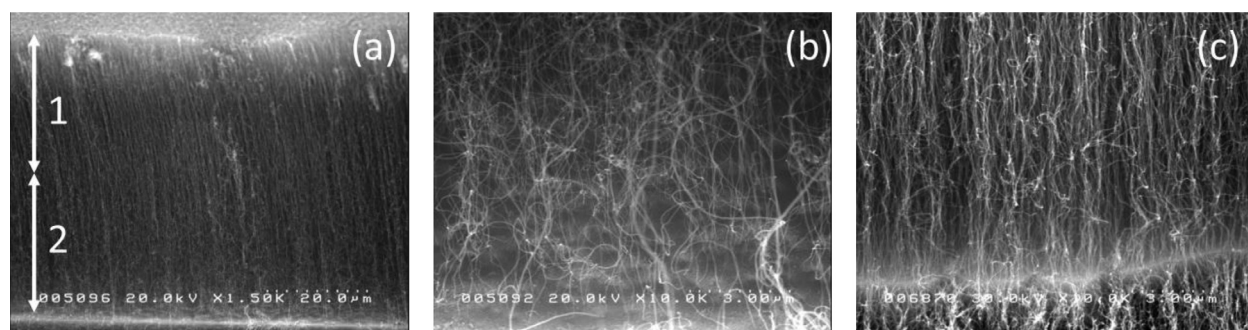FIG. 4. Two-layer CNT forest growth on quartz at 700 °C. First layer was grown by 1.5 mol. % ferrocene/xylene injected at 2 ml/h for a total of 0.5 ml with a carrier gas mixture of H$_2$:Ar = 50:50 sccm followed by a second layer grown by 20 min of gas mixture C$_2$H$_4$: H$_2$: Ar = 10:40:50 sccm. (a) Side view of the forest. The first layer (denoted by 1) is more aligned than the second layer (denoted by 2). (b) Base region of the second layer. (c) Base region of a ferrocene/xylene growth under the same condition as the first layer in (a).

the precursor can be compensated by a higher injection rate, but one has to be concerned with the total carbon concentration in the reactor. If the decomposition rate of carbon feedstock is higher than the carbon precipitation rate, excessive carbon deposition on the nanoparticles can be detrimental to their catalytic activity and lead to early growth termination. CNT density increasing with ferrocene concentration was also observed by Castro *et al.*[41] However, they reported a significant decrease of the average outer diameter with increasing ferrocene concentration, which is opposite to a significant increase of the outer diameter observed by Singh *et al.*[4] Our SEM top-view images which represent the morphology of the initial CNT growth do not show any significant CNT size difference from a ferrocene concentration of 1.5% to 7.2% by an injection rate of 2 ml/h on quartz at 700 °C. However, given the difficulty of sampling different tubes in a crust to make valid statistical analysis of their diameters, we do not have any quantitative conclusion at this point.

C. Forest height is limited by density

It has been generally accepted that catalyst particles created from a thin layer (≤ 1 nm) of metal on oxide surfaces do not form a CNT forest dense enough to be terminated by cutting off the supply of a carbon feedstock like CH_4, C_2H_2, or C_2H_4. Rather, the forest growth is terminated by the disappearing of the nanoparticles or losing the catalytic function of the nanoparticles. Therefore, to achieve super-long CNTs, one has to choose an underlayer that can prevent catalyst diffusion and an oxidant to extend catalyst lifetime and CNT growth rate. However, as described in Sec. III B, using injection CVD the ferrocene concentration in a precursor can be so high that precursor diffusion indeed limits the forest growth. By using a precursor injection rate of 2 ml/h, a precursor volume of 0.5 ml and temperature at 700 °C, we find that the range of CNT forest height on quartz is 12–18, 10, and 5–7 μm for 1.5, 3, and 6 mol. % of ferrocene precursor, respectively. The SEM images clearly show that there are more particles and entanglement near the top for the 3 and 6 mol. % samples than the 1.5% samples. When the ferrocene concentration was raised to 7.2 mol. %, we obtained a mere 1–2 μm high forest with very dense and thick tubes decorated with particles near the top region as shown in Fig. 6. Even a higher growth temperature (760 °C) did not dilute the density. Note that higher ferrocene concentration does not change much of the carbon supply rate, because xylene is the main carbon source. By keeping a constant precursor injection rate, gas mixture, and temperature, we believe that the lifetime of the catalyst particles and CNT growth rate should remain constant. These results indicate that the culprit of early growth termination in our case is diffusion.

As discussed in Sec. III A, the CNT forests are much denser on sapphire substrates than on quartz or silicon oxide substrates grown under the same conditions. As a result of the diffusion limit, the forest heights on sapphire are substantially lower than those on quartz (and silicon oxide) for all growth conditions as shown unequivocally in Fig. 2.
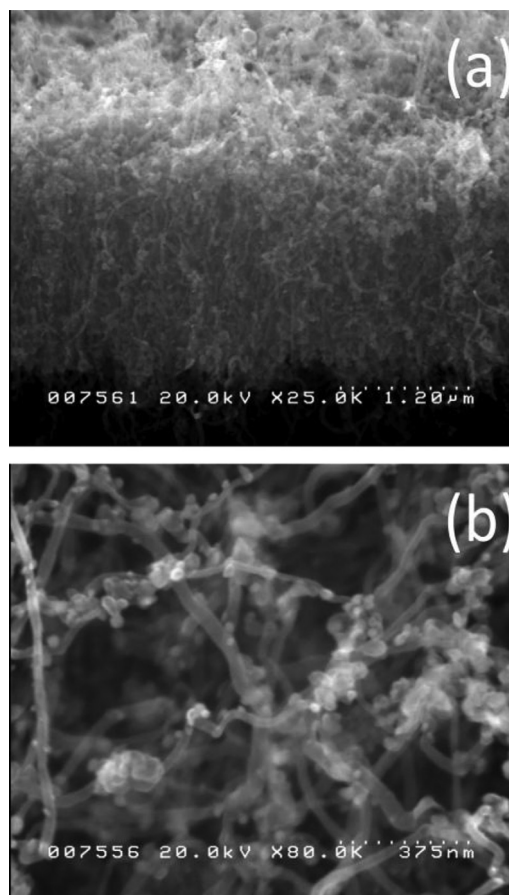

FIG. 6. CNT forest grown by 7.2 mol. % ferrocene/xylene injected at 4 ml/h for a total of 0.5 ml at 760 °C. The carrier gas mixture was H_2:Ar = 52.5:47.5 sccm. (a) Side view of a piece of the forest. (b) Close-up image of the CNTs (top view).

The CNT forest may present a significant diffusion barrier for larger molecules. The particles on the top part of the CNTs shown in Fig. 6(b) were also observed in Ref. 1 where they are attributed to the carbon coating from thermally decomposed hydrocarbon molecules. The fact that their concentration decreased toward the base is another indication of the diffusion limit. Furthermore, the pyrolysis of xylene and ferrocene can generate benzene and other high melting point polycyclic aromatic hydrocarbons (PAHs).[56] Without a proper concentration of H_2 to reduce the PAH yield, the PAHs could be trapped by the forest and form an reflective film on the top part of the forest after cooling down as well as an oily coating on the reactor wall observed early on.[57]

D. The effect of growth temperature and hydrogen concentration

Higher temperature promotes all chemical and physical processes such as hydrocarbon decomposition, CNT nucleation and growth, and catalyst evolution. As a result, forest height increased significantly from 700 °C to 760 °C as shown in Figs. 7(a) and 7(b). In particular, we observed that the CNT forest growth rate is very sensitive to hydrogen concentration in the carrier gas at 760 °C but not at 700 °C. The same behavior was observed on both quartz and sapphire
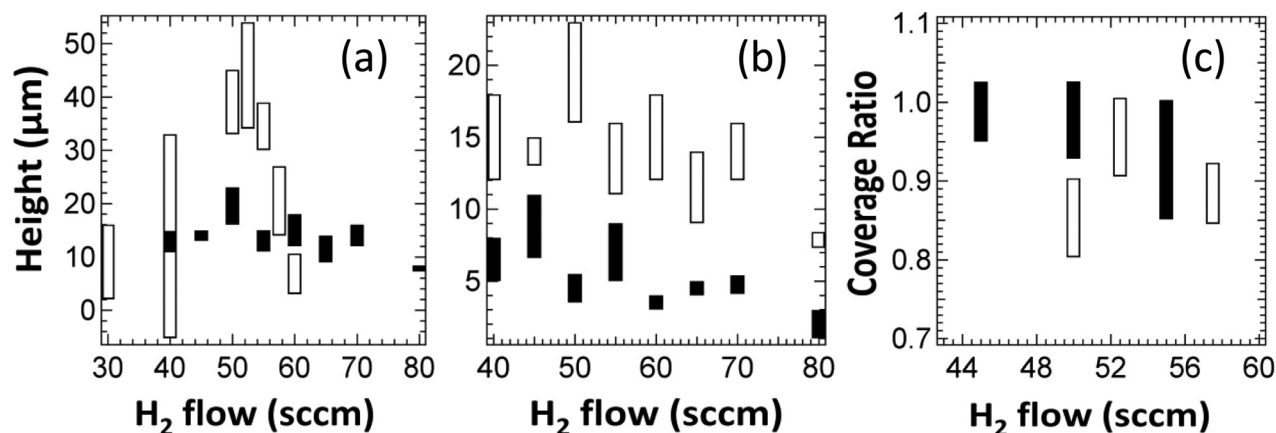
FIG. 7. (a) CNT forest height grown at 760 °C (open) and 700 °C (filled) on quartz for different H_2:Ar ratios in the carrier gas. The total flow rate was kept at 100 sccm. The precursor was 1.5 mol. % ferrocene/xylene injected at 2 ml/h at 700 °C and at 4 ml/h at 760 °C for a total of 0.5 ml. (b) Same conditions as (a) but on sapphire. (c) The ratio of percentage coverage at base to tip for the same conditions as (a) on quartz.

substrates. We do not observe a significant tip density difference at these two temperatures, but the base density is significantly lower at 760 °C [Fig. 1(c)] than at 700 °C [Fig. 4(c)]. A comparison of the base to tip density ratio at these two temperatures with different H_2 concentration is depicted in Fig. 7(c). The drastic reduction of the CNT density near the base at higher temperatures can be explained by the lift-up scenario discussed earlier enhanced by a shorter catalyst lifetime except at an optimal hydrogen mixture. Although the notion that higher temperature enhances CNT growth rate but reduces catalyst lifetime by a higher carbon deposition rate has been pointed out recently,[42,58] we would like to point out that the higher growth rate may be offset by the adhesion loss from lift-up effect for many applications. More on this is discussed in Sec. IV.

Hydrogen can play several competing roles in CNT synthesis by CVD. In the case of CH_4-CVD, Franklin *et al.* reported that insufficient H_2 causes vigorous pyrolysis resulting in amorphous carbon poisoning catalyst particles and higher hydrocarbon generation, while too much H_2 reduces the rate of CH_4 decomposition and CNT yields.[57] This description matches our observation of the ferrocene/xylene-CVD. To verify the role of hydrogen, we injected pure xylene into the CVD reactor at 700 °C while maintaining the total flow rate of the carrier gas at 100 sccm. We find that reddish droplets precipitated at the exhaust end of the reactor when the xylene injection rate was 4 ml/h with a gas mixture of H_2:Ar = 25:75. The reddish droplets reduced to yellow mist either by increasing the H_2 concentration to 50 sccm or reducing the xylene flow rate to 2 ml/h. We cannot eliminate the possibility that our ultrapure hydrogen has trace amounts of water and oxygen which enhances catalyst lifetime and growth rate as demonstrated by In *et al.*[45] but the clear enhancement of the hydrogen effect at higher temperature, the observation of PAH/higher hydrocarbon formation at lower hydrogen concentration, and reduced growth at higher hydrogen concentration emphasize the role of H_2 in precursor pyrolysis. It is worthwhile to note that there have been reports of growing CNT forests by liquid precursors such as xylene, toluene, or benzene without introducing H_2.[40,42,43] It

is hard to compare these results given the very different carrier flow rate, precursor injection rate, and the possibility of oxidant impurities in the gas mixture. However, the much thicker CNT diameters and particles on the tube wall presented in these references seems to suggest a much stronger pyrolysis in the low H_2 limit.

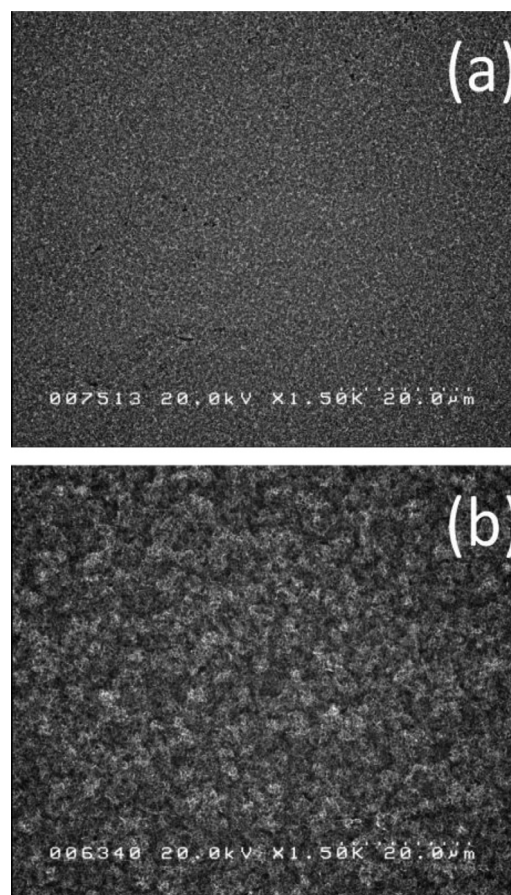Note that hydrogen is also important for pre-deposited catalyst CVD but for different reasons. In that case, the

FIG. 8. CNT forest grown by 1.5 mol. % ferrocene/xylene injected at 4 ml/h at (a) 700 °C (b) 760 °C. The carrier gas mixture was H_2:Ar = 50:50 sccm.

catalyst film is usually exposed to air before moving to the CVD chamber. Therefore, it is critical to use H_2 or NH_3 to activate the nanoparticles by reducing their oxide.[18,59] Additionally, Nessim *et al.* found that reduced Fe particles can agglomerate which leads to slower CNT growth but without introducing H_2 leads to poor growth in C_2H_4-CVD.[60]

Zhang *et al.* proposed the crust scenario to explain why all the CNTs appear to have the same length in a forest.[53] As soon as the entanglement of the crust creates a strong lateral hindrance, the CNT growth proceeds with vertical alignment. In injection CVD this scenario also holds at 700 °C as as shown in Fig. 8(a) where the surfaces of the forests are quite smooth. The newly nucleated CNTs grow roughly at the same rate as the existing CNTs. However, at high temperatures the CNT growth is faster which increases the inhomogeniety of the catalyst nucleation leading to the formation of local crusts and uneven height across the whole forest surface as shown in Fig. 8(b).

IV. CONCLUSIONS

We present an integrated scenario on controlling the density of the forest by injection CVD. The primary factor is the diffusion rate of catalyst adatoms on and into the substrate at the growth temperature. Based on the catalyst diffusion rate, the concentration of the ferrocene in the solvent and the precursor injection rate can be optimized. A high density of catalyst particles can create a significant diffusion barrier for the precursor molecule to reach the catalyst particles while a low density of catalyst particles will not form vertically aligned CNTs. To promote thermal decomposition of the precursor molecules and suppress the pyrolysis of PAH and higher hydrocarbons, a proper amount of H_2 in the reactor is necessary. Too much hydrogen will reduce the CNT growth by suppressing the dehydrogenation reactions. Higher temperatures promote all chemical reactions including hydrocarbon decomposition and CNT precipitation. However, excessive carbon could reduce catalyst lifetime. Due to the lift-up effect, continuous nucleation of new catalyst particles in injection CVD could in principle lead to unlimited growth, if the catalyst nucleation rate balances the catalyst inactivation rate. However, the diffusion barrier created by the forest eventually will stop the carbon supply and terminate the growth. Therefore, increasing the growth rate by introducing a proper amount of oxidant is necessary.[1]

From the CNT yield point of view, C_2H_2 as a carbon source is clearly superior to xylene based on the study of Eres *et al.*[61] and many growth rates reported in the literature. However, for many applications adhesion to the substrate is also important. Since the lift-up effect leads to reduced density toward the base, the adhesion of the forest to the substrate is greatly reduced. We noticed that after switching the carbon feedstock from ferrocene/xylene precursor to C_2H_4 gas, CNT density near the base is drastically reduced and the forest can be easily blown off by a stream of N_2 gas. In contrast, forests grown by a properly concentrated ferrocene/xylene solution can maintain the density from tip to base and the forest is robust enough to be cleaned by N_2 gas. Alternatively, by using an abrupt termination technique, Liu *et al.*

reported that the adhesion of C_2H_2-CVD grown CNT forests with the substrate can be improved by a factor of 3 higher than the adhesion by the naturally terminated forests.[49] However, this method only works if the growth is terminated before a significant lift-off starts, so the majority of the CNTs are still in contact with the substrate. In contrast, injection CVD can maintain the CNT film adhesion until the growth is terminated by diffusion.

[1]X. Li, X. Zhang, L. Ci, R. Shan, C. Wolfe, S. Kar, S. Talapatra, and P. M. Ajayan, Nanotechnology **19**, 455609 (2008).

[2]S. Yasuda, D. N. Futaba, T. Yamada, J. Satou, A. Shibuya, H. Takai, K. Arakawa, M. Yumura, and K. Hata, ACS Nano **3**, 4164 (2009).

[3]C. J. Lee and J. Park, Appl. Phys. Lett. **77**, 3397 (2000).

[4]C. Singh, M. S. P. Shaffer, and A. H. Windle, Carbon **41**, 359 (2003).

[5]H. M. Cheng, F. Li, G. Su, H. Y. Pan, L. L. He, X. Sun, and M. S. Dresselhaus, Appl. Phys. Lett. **72**, 3282 (1998).

[6]R. Kamalakaran, M. Terrones, T. Seeger, Ph. Kohler-Redich, M. Ruhle, Y. A. Kim, T. Hayashi, and M. Endo, Appl. Phys. Lett. **77**, 3385 (2000).

[7]M. Pinault, V. Pichot, H. Khodja, P. Launois, C. Reynaud, and M. Mayne-L'Hermite, Nano Lett. **5**, 2394 (2005).

[8]I. Kunadian, R. Andrews, D. Qian, and M. P. Menguc, Carbon **47**, 384 (2009).

[9]Ch. Emmenegger, P. Mauron, A. Zuttel, Ch. Nutzenadel, A. Schneuwly, R. Gallay, and L. Schlapbach, Appl. Surf. Sci. **162–163**, 452 (2000).

[10]S. Sakurai, H. Nishino, D. N. Futaba, S. Yasuda, T. Yamada, A. Maigne, Y. Matsuo, E. Nakamura, M. Yumura, and K. Hata, J. Am. Chem. Soc. **134**, 2148 (2012).

[11]S. S. Lee, C. Zhang, Z. A. Lewicka, M. Cho, J. T. Mayo, W. W. Yu, R. H. Hauge, and V. L. Colvin, J. Phys. Chem. C **116**, 10287 (2012).

[12]C. Bower, O. Zhou, W. Zhu, D. J. Werder, and S. Jin, Appl. Phys. Lett. **77**, 2767 (2000).

[13]M. Chhowalla, K. B. K. Teo, C. Ducati, N. L. Rupesinghe, G. A. J. Amaratunga, A. C. Ferrari, D. Roy, J. Robertson, and W. I. Milne, J. Appl. Phys. **90**, 5308 (2001).

[14]Y. Y. Wei, G. Eres, V. I. Merkulov, and D. H. Lowndes, Appl. Phys. Lett. **78**, 1394 (2001).

[15]S. Wei, W.P. Kang, J. L. Davidson, and J. H. Huang, Diamond Relat. Mater. **15**, 1828 (2006).

[16]P. B. Amama, C. L. Pint, L. McJilton, S. M. Kim, E. A. Stach, P. T. Murray, R. H. Hauge, and B. Maruyma, Nano Lett. **9**, 44 (2009).

[17]N. R. Franklin, Y. Li, R. J. Chen, A. Javey, and H. Dai, J. Phys. Chem. B **105**, 11424 (2001).

[18]G. S. Choi, Y. S. Cho, S. Y. Hong, J. B. Park, K. H. Son, and D. J. Kim, J. Appl. Phys. **91**, 3847 (2002).

[19]D. N. Futaba, K. Hata, T. Namai, T. Yamada, K. Mizuno, Y. Hayamizu, M. Yumura, and S. Iijima, J. Phys. Chem. B **110**, 8035 (2006).

[20]K. Hata, D. N. Futaba, K. Mizuno, T. Namai, M. Yumura, and S. Lijima, Science **306**, 1362 (2004).

[21]C. Mattevi, C. T. Wirth, S. Hofmann, R. Blume, M. Cantoro, C. Ducati, C. Cepek, A. Knop-Gericke, S. Milne, C. Castellarin-Cudia, S. Dolafi, A. Goldoni, R. Schloegl, and J. Robertson, J. Phys. Chem. C **112**, 12207 (2008).

[22]D. N. Futaba, J. Goto, S. Yasuda, T. Yamada, M. Yumura, and K. Hata, Adv. Mater. **21**, 4811 (2009).

[23]S. M. Kim, C. L. Pint, P. B. Amama, R. H. Hauge, B. Maruyma, and E. A. Stach, J. Mater. Res. **25**, 1875 (2010).

[24]S. Oida, F. R. McFeely, and A. A. Bol, J. Appl. Phys. **109**, 064304 (2011).

[25]K. Hasegawa and S. Noda, ACS Nano **5**, 975 (2011).

[26]R. Guzmán de Villoria, A. J. Hart, and B. L. Wardle, ACS Nano **5**, 4850 (2011).

[27]R. Sen, A. Govindaraj, and C. N. R. Rao, Chem. Phys. Lett. **267**, 276 (1997).

[28] R. Andrews, D. Jacques, A. M. Rao, F. Derbyshire, D. Qian, X. Fan, E. C. Dickey, and J. Chen, Chem. Phys. Lett. **303**, 467 (1999).

[29] C. P. Deck and K. Vecchio, Carbon **44**, 267 (2006).

[30] L. M. Dyagileva, V. P. Mar'in, E. I. Tsyganova, and G. A. Razuvaev, J. Organomet. Chem. **175**, 63 (1979).

[31] K. Kuwana, H. Endo, K. Saito, D. Qian, R. Andrews, and E. A. Grulke, Carbon **43**, 253 (2005).

[32] D. M. Matheu, A. M. Dean, J. M. Grenda, and W. H. Green, Jr., J. Phys. Chem. A **107**, 8552 (2003).

[33] X. Zhang, A. Cao, B. Wei, Y. Li, J. Wei, C. Xu, and D. Wu, Chem. Phys. Lett. **362**, 285 (2002).

[34] L. Zhang and D. E. Resasco, Langmuir **25**, 4792 (2009).

[35] T. Tong, Y. Zhao, L. Delzeit, A. Kashani, M. Meyyappan, and A. Majumdar, IEEE Trans. Compon. Packag. Technol. **30**, 92 (2007).

[36] K. Mizuno, J. J. Ishii, H. Kishida, Y. Hayamizu, S. Yasuda, D. N. Futaba, M. Yumura, and K. Hata, Proc. Nat. Acad. Sci. U.S.A. **106**, 6044 (2009).

[37] L. Qu, L. Dai, M. Stone, Z. Xia, and Z. L. Wang, Science **322**, 238 (2008).

[38] B. L. Wardle, D. S. Saito, E. J. García, A. J. Hart, R. Guzmán de Villoria, and E. A. Verploegen, Adv. Mater. **20**, 2707 (2008).

[39] K. Gong, F. Du, Z. Xia, M. Durstock, and L. Dai, Science **323**, 760 (2009).

[40] L. Tapasztó, K. Kertész, Z. Vértesy, Z. E. Horváth, A. A. Koós, Z. Osváth, Zs. Sárközi, Al. Darabont, and L. P. Biró, Carbon **43**, 970 (2005).

[41] C. Castro, M. Pinault, S. Coste-Leconte, D. Porterat, N. Bendiab, C. Reynaud, and M. Mayne-L'Hermite, Carbon **48**, 3807 (2010).

[42] M. I. Ionescu, Y. Zhang, R. Li, X. Sun, H. Abou-Rachid, and L.-S. Lusssier, Appl. Surf. Sci. **257**, 6843 (2011).

[43] J. R. Raney, A. Misra, and C. Daraio, Carbon **49**, 3631 (2011).

[44] M. Bedewy, E. R. Meshot, M. J. Reinker, and A. J. Hart, ACS Nano **5**, 8974 (2011).

[45] J. B. In, C. P. Grigoropoulos, A. A. Chernov, and A. Noy, Appl. Phys. Lett. **98**, 153102 (2011); ACS Nano **5**, 9602 (2011).

[46] J. J. Jackson, A. A. Puretzky, K. L. More, C. M. Rouleau, G. Eres, and D. B. Geohegan, ACS Nano **4**, 7573 (2010).

[47] H. Ohno, D. Takagi, K. Yamada, S. Chiashi, A. Tokura, and Y. Homma, Jpn. J. Appl. Phys. **47**, 1956 (2008).

[48] J.-T. Di, Z.-Z. Yong, X.-J. Yang, and Q.-W. Li, Appl. Surf. Sci. **258**, 13 (2011).

[49] K. Liu, K. Jiang, Y. Wei, S. Ge, P. Liu, and S. Fan, Adv. Mater. **19**, 975 (2007).

[50] R. Xiang, G. Luo, W. Qian, Q. Zhang, Y. Wang, F. Wei, Q. Li, and A. Cao, Adv. Mater. **19**, 2360 (2007).

[51] A. Cao, P. M. Ajayan, G. Ramanath, R. Baskaran, and K. Turner, Appl. Phys. Lett. **84**, 109 (2004).

[52] R. Xiang, G. Luo, Z. Yang, Q. Zhang, W. Qian, and F. Wei, Nanotechnology **18**, 415703 (2007).

[53] L. Zhang, Z. Li, Y. Tan, G. Lolli, N. Sakulchaicharoen, F. G. Requejo, B. S. Mun, and D. E. Resasco, Chem. Mater. **18**, 5624 (2006).

[54] E. R. Meshot and A. J. Hart, Appl. Phys. Lett. **92**, 113107 (2008).

[55] H. Wang, Z. Xu, and G. Eres, Appl. Phys. Lett. **88**, 213111 (2006).

[56] C. T. Brooks, S. J. Peacock, and B. G. Reuben, J. Chem. Soc., Faraday Trans. **75**, 652 (1979).

[57] N. R. Franklin, Y. Li, R. J. Chen, A. Javey, and H. Dai, Appl. Phys. Lett. **79**, 4571 (2001).

[58] K. Hasegawa and S. Noda, Carbon **49**, 4497 (2011).

[59] S. Esconjauregui, M. Fouquet, B. C. Bayer, S. Eslava, S. Khachadorian, S. Hofmann, and J. Robertson, J. Appl. Phys. **109**, 044303 (2011).

[60] G. D. Nessim, A. J. Hart, J. S. Kim, D. Acquaviva, J. Oh, C. D. Morgan, M. Seita, J. S. Leib, and C. V. Thompson, Nano Lett. **8**, 3587 (2008).

[61] G. Eres, A. A. Kinkhabwala, H. Cui, D. B. Geohegan, A. A. Puretzky, and D. H. Lowndes, J. Phys. Chem. B **109**, 16684 (2005).